



Full length article

# Quantum and thermal pressures from light scalar fields

 Hauke Fischer<sup>1</sup>, Christian Käding<sup>1\*</sup>, Mario Pitschmann<sup>1</sup>

Atominstitut, Technische Universität Wien, Stadionallee 2, 1020 Vienna, Austria

## ARTICLE INFO

### Keywords:

 Dark energy  
 Screened scalar fields  
 Quantum pressure  
 Thermal pressure

## ABSTRACT

Light scalar fields play a variety of roles in modern physics, especially in cosmology and modified theories of gravity. For this reason, there is a zoo of experiments actively trying to find evidence for many scalar field models that have been proposed in theoretical considerations. Among those are setups in which the pressures expected to be induced by light scalar fields between two parallel plates are studied, for example, Casimir force experiments. While it is known that classical and quantum pressures caused by light scalar fields could have significant impacts on such experiments, in this article, we show that this can also be the case for thermal pressure. More specifically, we derive expressions for the quantum and thermal pressures induced by exchanges of light scalar field fluctuations between two thin parallel plates. As particular examples, we then look at screened scalar fields. For chameleon, symmetron and environment-dependent dilaton models, we find large regions in their parameter spaces that allow for thermal pressures to equal or exceed the quantum pressures. By comparing with earlier constraints from quantum pressure calculations, we conclude that thermal pressures induced by chameleons are actually of experimental significance.

## 1. Introduction

Light scalar fields appear in many contexts in modern cosmology or modifications of general relativity, for example, in scalar-tensor theories of gravity [1]. They often serve as the basis for proposed solutions of some of modern physics' greatest open problems, including dark energy (DE) and dark matter (DM) [2,3]. Many of such theories give rise to a universal coupling between the scalar degree of freedom and Standard Model matter, leading to an additional force of Nature. Such a fifth force, however, is tightly constrained within our Solar System [4–6].

Screening mechanisms were devised to provide a way of circumventing these constraints while also offering a rich phenomenology. They strongly suppress (screen) scalar fifth forces in environments of sufficiently high mass densities, e.g., our Solar System, but enable them to develop their full strengths in regions of lower densities. There are a variety of different light scalar field models with screening mechanisms, so-called screened scalar fields, some of which are even being discussed as presenting an alternative to particle DM through their fifth forces [7–10]. Some of the most popular screened scalar field models are chameleons [11,12], symmetrons [13–20], and environment-dependent dilatons [15,18,21–25]. They are the examples used in the present article, and have already been tested and discussed in multiple experimental setups; see, e.g., Refs. [26–61]. For an overview of current constraints on the parameter spaces of these models, see Refs. [62,63].

While screened scalar fields are usually treated as classical fields, there have already been first attempts to describe them in quantum field theoretical frameworks [64–67] and from the perspective of particle physics [68]. The present article will add to this.

Casimir force experiments like the upcoming *Casimir And Non Newtonian force EXperiment* (CANNEX) [58,69] are expected to further constrain the parameter spaces of light scalar field models [54,70–73]. This makes this type of experiments an interesting subject for theoretical analyses and motivates the investigation in the present article. Ref. [64] initiated the discussion of quantum pressure induced between two parallel plates, as can be found in CANNEX, by interactions with quantum fluctuations of screened scalar fields. For this, the plates were approximated by having infinite widths and infinite thicknesses. Using this approximation, Ref. [64] showed that the quantum pressures of chameleons and symmetrons can actually be quite significant and lead to tighter constraints on these models' parameter spaces. In the present article, we consider two equal, infinitely wide, but very thin plates and also study the quantum pressures induced by light scalar fields, while considering chameleons, symmetrons, and environment-dependent dilatons as representative examples. In order to obtain analytically tractable results, we restrict our analysis to parameter regimes in which these screened scalar fields have Compton wavelengths much larger than the thickness of one plate. This means that throughout our investigation, we can safely assume the scalar fields to have constant

\* Corresponding author.

E-mail addresses: [hauke.fischer@tuwien.ac.at](mailto:hauke.fischer@tuwien.ac.at) (H. Fischer), [christian.kaeding@tuwien.ac.at](mailto:christian.kaeding@tuwien.ac.at) (C. Käding), [mario.pitschmann@tuwien.ac.at](mailto:mario.pitschmann@tuwien.ac.at) (M. Pitschmann).

<https://doi.org/10.1016/j.dark.2024.101756>

Received 30 July 2024; Received in revised form 4 November 2024; Accepted 26 November 2024

Available online 9 December 2024

2212-6864/© 2024 The Authors. Published by Elsevier B.V. This is an open access article under the CC BY license (<http://creativecommons.org/licenses/by/4.0/>).

masses defined by the density of the vacuum surrounding the plates. Consequently, the general parts of our results are applicable to any type of scalar field model that exhibits a constant mass in the considered situation. Motivated by the results of Refs. [65–67], which indicated that finite-temperature effects of light scalar fields could be relevant for experiments, we also compute expressions for the pressures induced by thermal scalar fluctuations. Comparing the results for quantum and thermal pressures, we find that both can be of comparable magnitudes in some situations. Due to the proven significance of quantum pressures according to Ref. [64], we consequently conclude that thermal pressures are likely also relevant for screened scalar field models in some experimental setups and must therefore be taken into account.

This article is structured as follows: At first, in Section 2, we shortly introduce the three considered screened scalar field models and discuss their couplings to fermions. Next, in Section 3, we compute the quantum and thermal potentials, and derive and discuss the resulting pressures between two parallel plates. Finally, we draw our conclusions in Section 4.

## 2. Scalar field models

While it should be noted that some of the main results in this article are applicable to more general types of light scalar fields, we will use three popular types of screened scalar fields models as examples for our discussion. In this way, we are able to make comparisons with the results of Ref. [64]. Therefore, in this section, we first give a short overview of the considered screened scalar field models and provide all necessary formulas. Afterwards, we discuss the couplings of the scalar fields to fermions since they are required for the computations done in this article.

### 2.1. Models

As examples, we consider three screened scalar field models: chameleons, symmetrons, and environment-dependent dilatons. Each of them can be generally described by the Einstein frame action

$$S = \int d^4x \sqrt{-g} \left( -\frac{m_{\text{Pl}}^2}{2} R + \frac{1}{2} (\partial\varphi)^2 - V_X(\varphi) \right) + \int d^4x \sqrt{-\tilde{g}^X} \mathcal{L}_{\text{SM}}(\tilde{g}_{\mu\nu}^X, \psi_i), \quad (1)$$

in which  $m_{\text{Pl}}$  is the reduced Planck mass;  $\varphi$  represents the scalar field;  $X \in \{C, S, D\}$  labels the scalar field model, i.e., chameleon ( $C$ ), symmetron ( $S$ ), or dilaton ( $D$ );  $V_X(\varphi)$  is the scalar's potential; and  $\mathcal{L}_{\text{SM}}$  denotes a Lagrangian describing the Standard Model fields  $\psi_i$ . For notational convenience, in Eq. (1), we kept the Jordan frame metric defined in terms of the conformal factor  $A_X(\varphi)$  as  $\tilde{g}_{\mu\nu}^X = A_X^2(\varphi)g_{\mu\nu}$ . Due to the conformal factor, the scalar  $\varphi$  couples to the field  $\psi_i$ . In turn, this leads to an effective potential for the scalar:

$$V_{X:\text{eff}}(\varphi) := V_X(\varphi) + A_X(\varphi)T_\mu^\mu \quad (2)$$

with  $T_\mu^\mu$  as the trace of the energy momentum tensor of  $\psi_i$ .

For chameleons, we have

$$V_C = \frac{\Lambda^{n+4}}{\varphi^n}, \quad A_C(\varphi) = \exp\left(\frac{\varphi}{M_C}\right) \approx 1 + \frac{\varphi}{M_C} + \frac{\varphi^2}{2M_C^2}, \quad (3)$$

where  $n \in \mathbb{Z}^+ \cup 2\mathbb{Z}^- \setminus \{-2\}$  defines the exact chameleon model;  $\Lambda$  is a mass scale determining the chameleon's self-interaction, except for the case  $n = -4$ , in which case it must actually be a dimensionless constant; and  $M_C$  is another mass scale, which controls the chameleon coupling to matter. Here, we have assumed  $\varphi \ll M_C$  and kept the second order term in order to allow for comparisons with symmetron and dilaton models. If we only consider the conformal factor up to the first order in  $\varphi/M_C$ , the effective potential defined by Eqs. (2) and (3) gives rise to an effective chameleon mass

$$m_C^2 = \frac{n(n+1)\Lambda^{n+4}}{\varphi^{n+2}} \quad (4)$$

with the chameleon vacuum expectation value (VEV) given by

$$\varphi_C = \left( n\Lambda^{n+4} \frac{M_C}{T_\mu^\mu} \right)^{1/(n+1)}. \quad (5)$$

While we have kept the second order term of the conformal factor in Eq. (3) in order to enable us to discuss the exchange of two chameleon field fluctuations, the second order corrections to Eqs. (4) and (5) are not relevant in the following discussions. Clearly, for any permitted value of  $n$ , a larger  $T_\mu^\mu$  implies a larger  $m_C$  in Eq. (4). Considering the example of non-relativistic matter, this means that a quantum of a chameleon field is the heavier the denser its surrounding environment it couples to. A heavier chameleon induces a shorter-ranged fifth force. This is the essence of the chameleon screening mechanism [11,12].

The symmetron model is defined by

$$V_S = -\frac{\mu^2}{2} \varphi^2 + \frac{\lambda_S}{4} \varphi^4, \quad A_S(\varphi) = 1 + \frac{\varphi^2}{2M_S^2} \quad (6)$$

with the tachyonic mass  $\mu$ , the dimensionless self-coupling parameter  $\lambda_S$ , and the mass scale  $M_S$  defining the symmetron's coupling to matter. It is screened by the Damour–Polyakov mechanism [15], which means that the symmetron's effective coupling to matter varies with the density of the environment. In the case  $T_\mu^\mu \geq \mu^2 M_S^2$ , the symmetron VEV must vanish, which results in a complete decoupling from matter if quantum or thermal fluctuations of the symmetron are small enough to be ignored. However, if  $T_\mu^\mu < \mu^2 M_S^2$ , the symmetron has a non-vanishing VEV

$$\varphi_S = \pm \sqrt{\frac{1}{\lambda_S} \left( \mu^2 - \frac{T_\mu^\mu}{M_S^2} \right)}, \quad (7)$$

which implies that the symmetron fifth force is unscreened. The symmetron mass is given by

$$m_S^2 = \begin{cases} \frac{T_\mu^\mu}{M_S^2} - \mu^2 & , T_\mu^\mu \geq \mu^2 M_S^2 \\ 2 \left( \mu^2 - \frac{T_\mu^\mu}{M_S^2} \right) & , T_\mu^\mu < \mu^2 M_S^2 \end{cases}. \quad (8)$$

Note that the symmetron also has an environment-dependent mass and is therefore, technically, a chameleon as well. However, the variation of the effective mass usually has only little influence on the fifth force screening of this model.

Finally, the environment-dependent dilaton has

$$V_D = V_0 e^{-\lambda\varphi/m_{\text{Pl}}}, \quad A_D(\varphi) = 1 + A_2 \frac{\varphi^2}{2m_{\text{Pl}}^2}, \quad (9)$$

where  $V_0$  is a constant energy density,  $\lambda$  denotes the dilaton's dimensionless self-coupling constant, and  $A_2$  is a dimensionless constant determining the coupling to matter. Resulting from this, the dilaton has a VEV [25]

$$\varphi_D = \frac{m_{\text{Pl}}}{\lambda} W\left(\frac{\lambda^2 V_0}{A_2 T_\mu^\mu}\right) \quad (10)$$

with the Lambert  $W$ -function

$$W(x) = \sum_{n=1}^{\infty} \frac{(-n)^{n-1}}{n!} x^n. \quad (11)$$

Consequently, its mass is given by

$$m_D^2 = \frac{1}{m_{\text{Pl}}^2} \left( \lambda^2 V_0 e^{-\lambda\varphi_D/m_{\text{Pl}}} + A_2 T_\mu^\mu \right). \quad (12)$$

As can be inferred from Eq. (10), the dilaton VEV is the smaller the larger  $T_\mu^\mu$ . This means that, as long as any dilaton fluctuations are negligible, the coupling between dilaton and matter is small in dense environments. In turn, this leads to the dilaton fifth force being rendered weak in such environments. Initially, it was thought that the dilaton was only screened by this realization of the Damour–Polyakov mechanism. However, Ref. [54] showed that this is only partially true. In fact, there are only certain parts of the dilaton's parameter space in which the Damour–Polyakov mechanism is the dominant reason for fifth force screening. In other parameter regions, the dilaton fifth force is mainly screened by the chameleon mechanism.

## 2.2. Couplings to fermions

For the computations in this article, we will consider that the screened scalar fields couple to the nucleons in the two parallel plates. Consequently, we must describe the interactions between screened scalar fields and fermions.

From the effective actions of the considered models, we can conclude for the following interaction Lagrangians:

$$\begin{aligned}\mathcal{L}_{C:\text{int}} &= -\left(\frac{\varphi}{M_C} + \frac{\varphi^2}{2M_C^2}\right)T_\mu^\mu, \quad \mathcal{L}_{S:\text{int}} = -\frac{\varphi^2}{2M_S^2}T_\mu^\mu, \\ \mathcal{L}_{D:\text{int}} &= -A_2\frac{\varphi^2}{2m_{\text{Pl}}^2}T_\mu^\mu.\end{aligned}\quad (13)$$

We consider an interaction with a Dirac particle of mass  $m$  with stress–energy tensor

$$T_\nu^\mu = \bar{\psi}i\gamma^\mu\partial_\nu\psi - \bar{\psi}i\phi\psi\delta_\nu^\mu + m\bar{\psi}\psi\delta_\nu^\mu. \quad (14)$$

From this follows the trace

$$\begin{aligned}T_\mu^\mu &= -3\bar{\psi}i\phi\psi + 4m\bar{\psi}\psi \\ &= m\bar{\psi}\psi,\end{aligned}\quad (15)$$

where we have used the Dirac equation in the last step. After expanding the fields in terms of their VEVs and fluctuations  $\phi$ , such that  $\varphi = \varphi_X + \phi$ , we find that the Lagrangians in Eq. (13) give rise to interactions of fermions with one or two scalar fluctuations. This can be summarized in terms of two general interaction Lagrangians:

$$\mathcal{L}_{X:\text{int}}^{(1)} = -g_X^{(1)}\phi\bar{\psi}\psi, \quad \mathcal{L}_{X:\text{int}}^{(2)} = -g_X^{(2)}\phi^2\bar{\psi}\psi. \quad (16)$$

The dimensionless  $g_X^{(1)}$  are given by

$$g_C^{(1)} \approx \frac{m}{M_C}, \quad g_S^{(1)} = \frac{\varphi_S m}{M_S^2}, \quad g_D^{(1)} = \frac{A_2 \varphi_D m}{m_{\text{Pl}}^2}, \quad (17)$$

while the  $g_X^{(2)}$  have dimensions of an inverse mass and are

$$g_C^{(2)} = \frac{m}{2M_C^2}, \quad g_S^{(2)} = \frac{m}{2M_S^2}, \quad g_D^{(2)} = \frac{A_2 m}{2m_{\text{Pl}}^2}. \quad (18)$$

In Eq. (17), we have dropped the second order term of  $g_C^{(1)}$  since it will always be much smaller than the first order term. However, in order to also allow for a two-scalar exchange, we have kept the second order term that defines  $g_C^{(2)}$  in Eq. (18).

## 3. Quantum and thermal pressures

In this section, we compute the quantum and thermal pressures induced by light scalar fields between two infinitely wide, but very thin plates. For this, we first derive the quantum and thermal potentials from the interaction Lagrangians in Eq. (16). From those we then obtain the corresponding pressures. Finally, we compare quantum and thermal pressures in order to identify conditions for which both are of comparable magnitude. The obtained results are generally applicable to any scalar field model that has, in the considered experimental situation, a constant mass and couples to fermions as in Eq. (16).

Note that, for our examples of screened scalar fields, we assume a constant mass  $m_X$  throughout this discussion. This mass is defined only by the constant density of the vacuum or gas surrounding the two parallel plates. Such an assumption is well-justified as long as the Compton wavelength of a screened scalar field within one of the plates is much larger than the plate's thickness. In this case, the scalar field will not be able to minimize its potential within the plate. Conse-

quently, the density of the plate will only lead to small perturbations of the scalar's VEV and mass between the plates, which we can safely ignore. Certainly, this restricts the validity of the following discussion only to regions of the model parameter spaces that can comply with the requirements of our assumption.

### 3.1. Potentials

We have to consider the exchanges of one or two scalar fluctuations between two nucleons, one within one plate and one within the other plate. At first, we look at the single-particle exchange. In order to compute the quantum potential induced by light scalar fields from the interaction Lagrangian  $\mathcal{L}_X^{(1)}$  in Eq. (16), we follow Ref. [74]. Eq. (16) implies the scattering amplitude

$$i\mathcal{M}_{X:Q}^{(1)} = \left(ig_X^{(1)}\right)^2 \bar{u}(p'_2, \sigma_2)u(p_2, \sigma_2) \frac{i}{q^2 - m_X^2} \bar{u}(p'_1, \sigma_1)u(p_1, \sigma_1), \quad (19)$$

where the subscript  $Q$  indicates that we refer to the amplitude resulting from the quantum fluctuations of the scalar fields. In the non-relativistic limit, the amplitude takes the form

$$\mathcal{M}_{X:Q}^{(1)} = -\left(ig_X^{(1)}\right)^2 2m \frac{1}{q^2 + m_X^2} 2m. \quad (20)$$

A comparison with

$$\mathcal{M}_{X:Q}^{(1)} = -(2m)^2 V_{X:Q}^{(1)}(q), \quad (21)$$

where  $V_{X:Q}^{(1)}(q)$  is the Fourier transformed of the quantum potential  $V_{X:Q}^{(1)}(r)$ , yields immediately

$$V_{X:Q}^{(1)}(q) = -\left(g_X^{(1)}\right)^2 \frac{1}{q^2 + m_X^2}. \quad (22)$$

With the inverse Fourier transform

$$V_{X:Q}^{(1)}(r) = \int \frac{d^3q}{(2\pi)^3} V_{X:Q}^{(1)}(q) e^{iqr}, \quad (23)$$

we obtain the quantum potential for the single-scalar exchange:

$$V_{X:Q}^{(1)}(r) = -\left(g_X^{(1)}\right)^2 \frac{1}{4\pi r} e^{-m_X r}. \quad (24)$$

Next, we say that the thin parallel plates and the nucleons within them have a constant temperature  $T$ . Further, we follow Refs. [65–67] in assuming that the screened scalar field had sufficient time to thermalize with the plates, such that we can expect thermal scalar fluctuations associated with the temperature  $T$ . In this case, we can add a finite temperature contribution [75] to the propagator. However, as is explained below, the thermal contribution at tree level vanishes for kinematical reasons. In fact, the amplitude for the exchange of a single thermal scalar fluctuation between two nucleons is given by

$$i\mathcal{M}_{X:T}^{(1)} = \left(ig_X^{(1)}\right)^2 \bar{u}(p'_2, \sigma_2)u(p_2, \sigma_2) 2\pi\delta(q^2 - m_X^2) n(T, E_q) \bar{u}(p'_1, \sigma_1)u(p_1, \sigma_1), \quad (25)$$

where we use the Boltzmann distribution

$$n(T, E_q) = \exp(-E_q/T) \quad (26)$$

with energy  $E_q$ .<sup>1</sup> Though, since in the rest frame of a nucleon, i.e.,  $p_1 = (m, \mathbf{0})^T$ , we have

$$\begin{aligned}q^2 - m_X^2 &= (p_1 - p'_1)^2 - m_X^2 \\ &= 2m^2 - 2p_1 \cdot p'_1 - m_X^2 \\ &= 2m \left( m - \sqrt{m^2 + p_1'^2} \right) - m_X^2 < 0,\end{aligned}\quad (27)$$

relativistic invariance implies  $\delta(q^2 - m_X^2) = 0$  as well as  $\mathcal{M}_{X:T}^{(1)} = 0$ , as expected. This means that there are no thermal potential and pressure from a single-scalar exchange between two on-shell fermions.

<sup>1</sup> Note that we have approximated the Bose–Einstein distribution by the Boltzmann distribution for analytical reasons. This restricts our discussion to parts of the scalar field parameter spaces for which  $m_X \gg T$ .

For the quantum and thermal potentials from the two-scalar exchange, we take and validate the results from Ref. [75], which itself makes use of Refs. [76–78]. Therefore, for the quantum contribution, we find

$$V_{X;Q}^{(2)}(r) = - \left( g_X^{(2)} \right)^2 \frac{m_X}{8\pi^3 r^2} K_1(2m_X r). \quad (28)$$

Furthermore, for the thermal contribution, we obtain

$$V_{X;T}^{(2)}(r) = - \left( g_X^{(2)} \right)^2 \frac{1}{2\pi^3} \frac{1}{r} \frac{T m_X}{\sqrt{1 + (2rT)^2}} K_1 \left( \frac{m_X}{T} \sqrt{1 + (2rT)^2} \right). \quad (29)$$

It should be noted that this usual procedure of obtaining potentials implicitly assumes the nucleons to be on-shell, as is the case for free asymptotic scattering states. However, in the next section, we consider the case in which the nucleons are bound within the macroscopic plates. Hence, for our discussion, such a procedure of obtaining effective macroscopic potentials is an approximation.

### 3.2. Pressures

Having derived the quantum and thermal potentials between two nucleons, we can now use these results to compute the pressures between two parallel plates at separation  $\ell$ , with thicknesses  $D$  and widths  $2L$  in both transversal dimensions; see Fig. 1. The induced pressure between the two plates is computed by

$$P_{X;Y}^{(Z)}(\ell) = - \frac{\partial}{\partial \ell} \frac{\mathfrak{U}_{X;Y}^{(Z)}(\ell)}{S}, \quad (30)$$

where  $\mathfrak{U}_{X;Y}^{(Z)}(\ell)/S$  is the integrated potential per area  $S = 4L^2$  of both plates with  $Y \in \{Q, T\}$  and  $Z \in \{1, 2\}$ . We restrict our discussion to the case  $D \ll \ell$  and  $L \rightarrow \infty$ , and note that the results are only valid for parameters where  $D \ll 1/m_{X;\text{Plate}}$  is fulfilled. The last assumption corresponds to a field's Compton wavelength within a plate being much larger than the plate's thickness. In this case, the field cannot reach its VEV,  $\varphi_{X;\text{Plate}}$  within the plate but instead stays close to its VEV in vacuum,<sup>2</sup>  $\varphi_{X;\text{Vac}}$ . Consequently, we can safely assume that  $\varphi_{X;\text{Plate}} \approx \varphi_{X;\text{Vac}} =: \varphi_X$  and  $m_{X;\text{Plate}} \approx m_{X;\text{Vac}} =: m_X$ . In turn, the assumptions we make allow us to approximate the potential per area by

$$\frac{\mathfrak{U}_{X;Y}^{(Z)}(\ell)}{S} \approx \lim_{L \rightarrow \infty} \frac{D^2 \rho^2}{S} \int_{-L}^L dx \int_{-L}^L dx' \int_{-L}^L dy \times \int_{-L}^L dy' V_{X;Y}^{(Z)} \left( \sqrt{\ell^2 + (y' - y)^2 + (x' - x)^2} \right), \quad (31)$$

where the factor  $D^2$  stems from our approximation of the two integrals over the longitudinal direction,  $\rho$  is the nucleon number density of each plate,<sup>3</sup> and we set  $r = \sqrt{\ell^2 + (y' - y)^2 + (x' - x)^2}$ . We introduce new coordinates

$$x_{\pm} = x' \pm x, \quad y_{\pm} = y' \pm y. \quad (32)$$

Hence, we obtain

$$\begin{aligned} \frac{\mathfrak{U}_{X;Y}^{(Z)}(\ell)}{S} &\approx \lim_{L \rightarrow \infty} \frac{D^2 \rho^2}{4S} \int_{-2L}^{2L} dx_- \int_{|x_-| - 2L}^{2L - |x_-|} dx_+ \int_{-2L}^{2L} dy_- \int_{|y_-| - 2L}^{2L - |y_-|} dy_+ \\ &\times V_{X;Y}^{(Z)} \left( \sqrt{\ell^2 + y_-^2 + x_-^2} \right) \\ &\approx \lim_{L \rightarrow \infty} \frac{D^2 \rho^2}{S} \int_{-2L}^{2L} dx_- \int_{-2L}^{2L} dy_- (2L - |x_-|) (2L - |y_-|) \\ &\times V_{X;Y}^{(Z)} \left( \sqrt{\ell^2 + y_-^2 + x_-^2} \right). \end{aligned} \quad (33)$$

Taking the limit, we find

$$\begin{aligned} \frac{\mathfrak{U}_{X;Y}^{(Z)}(\ell)}{S} &\approx D^2 \rho^2 \int_{-\infty}^{\infty} dx_- \int_{-\infty}^{\infty} dy_- V_{X;Y}^{(Z)} \left( \sqrt{\ell^2 + y_-^2 + x_-^2} \right) \\ &\approx 2\pi D^2 \rho^2 \int_0^{\infty} d\tau \tau V_{X;Y}^{(Z)} \left( \sqrt{\ell^2 + \tau^2} \right). \end{aligned} \quad (34)$$

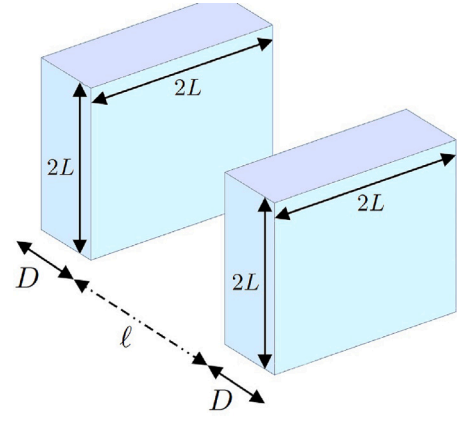


Fig. 1. Schematic depiction of the two parallel plates; the plates are identical in dimensions and material. We consider thin plates, which means that  $D \ll \ell$ . Furthermore, we take the limit  $L \rightarrow \infty$ . The plates are surrounded by vacuum or some kind of gas, and they themselves consist of a material with a density that leads to  $D \ll 1/m_{X;\text{Plate}}$  for the considered regions of the screened scalar fields models' parameter spaces.

Substituting  $v = \sqrt{\ell^2 + \tau^2}$ , we have

$$\frac{\mathfrak{U}_{X;Y}^{(Z)}(\ell)}{S} \approx 2\pi D^2 \rho^2 \int_{\ell}^{\infty} dv v V_{X;Y}^{(Z)}(v). \quad (35)$$

After substituting this into Eq. (30), we obtain

$$\begin{aligned} P_{X;Y}^{(Z)}(\ell) &\approx -2\pi D^2 \rho^2 \partial_{\ell} \int_{\ell}^{\infty} dv v V_{X;Y}^{(Z)}(v) \\ &\approx 2\pi D^2 \rho^2 \ell V_{X;Y}^{(Z)}(\ell). \end{aligned} \quad (36)$$

This means, from Eqs. (24), (28) and (29) we obtain:

$$P_{X;Q}^{(1)}(\ell) \approx - \left( g_X^{(1)} \right)^2 \frac{D^2 \rho^2}{2} e^{-m_X \ell}, \quad (37)$$

$$P_{X;Q}^{(2)}(\ell) \approx - \left( g_X^{(2)} \right)^2 \frac{m_X D^2 \rho^2}{4\pi^2 \ell} K_1(2m_X \ell), \quad (38)$$

$$P_{X;T}^{(2)}(\ell) \approx - \left( g_X^{(2)} \right)^2 \frac{D^2 \rho^2}{\pi^2} \frac{T m_X}{\sqrt{1 + (2\ell T)^2}} K_1 \left( \frac{m_X}{T} \sqrt{1 + (2\ell T)^2} \right). \quad (39)$$

Consequently, the total pressure, excluding pressures from classical fifth forces, induced by a scalar field of model  $X$  is given by

$$\begin{aligned} P_X(\ell) &= P_{X;Q}^{(1)}(\ell) + P_{X;Q}^{(2)}(\ell) + P_{X;T}^{(2)}(\ell) \\ &\approx -D^2 \rho^2 \left\{ \left( g_X^{(1)} \right)^2 \frac{1}{2} e^{-m_X \ell} + \left( g_X^{(2)} \right)^2 \frac{m_X}{\pi^2} \left[ \frac{1}{4\ell} K_1(2m_X \ell) \right. \right. \\ &\quad \left. \left. + \frac{T}{\sqrt{1 + (2\ell T)^2}} K_1 \left( \frac{m_X}{T} \sqrt{1 + (2\ell T)^2} \right) \right] \right\}. \end{aligned} \quad (40)$$

It should be noted, that each of the three pressure contributions, and as such the total pressure as well, are negative. This corresponds to an attractive force between the plates.

### 3.3. Discussion

We now discuss the regions of the considered screened scalar field models' parameter spaces where the induced thermal pressures are at least as large as the quantum pressures. This means that we are looking for model parameters that fulfill

$$\begin{aligned} \frac{\pi^2}{2} \left( \frac{g_X^{(1)}}{g_X^{(2)}} \right)^2 \frac{e^{-m_X \ell}}{m_X} + \frac{1}{4\ell} K_1(2m_X \ell) \\ \leq \frac{T}{\sqrt{1 + (2\ell T)^2}} K_1 \left( \frac{m_X}{T} \sqrt{1 + (2\ell T)^2} \right), \end{aligned} \quad (41)$$

where  $m_X \gg T$  due to our assumption of a Boltzmann distribution. In order to obtain quantitative results, we consider a plate separation of

<sup>2</sup> Here, the term vacuum also refers to any residual gases.

<sup>3</sup> We note, that the electron contributions can be safely neglected at our level of precision.

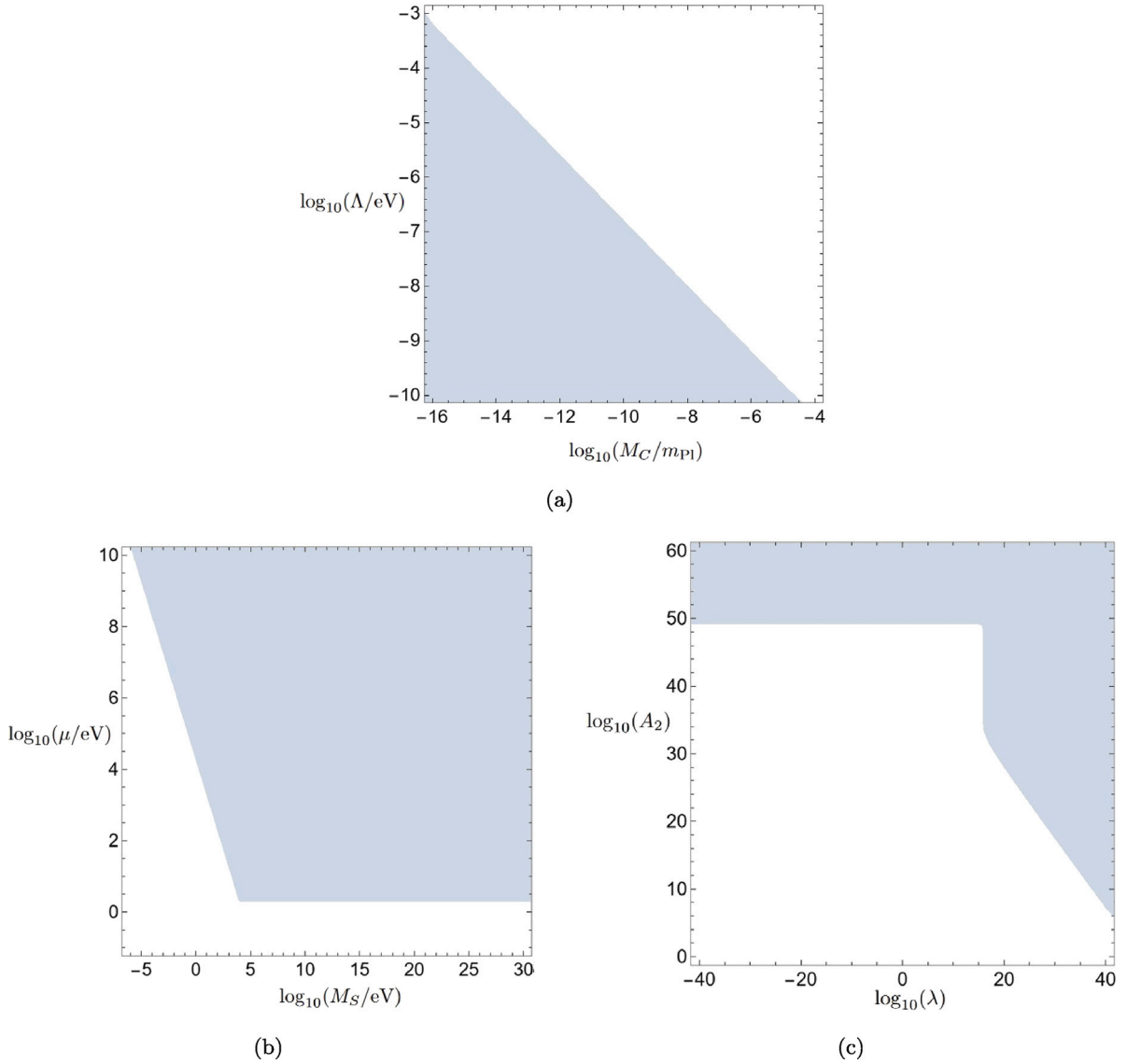


**Fig. 2.** Areas in the model parameter spaces for which Eq. (41) is valid for a hydrogen gas with  $T = 300$  K and a pressure of  $9.6 \times 10^{-10}$  mbar surrounding the two parallel plates; note that the plots continue where they touch one of the axes; (a): chameleon model with  $n = 1$ ; (b): symmetron in the symmetry-broken (unscreened) phase for  $\lambda_s = 0.1$ ; (c): environment-dependent dilaton with  $V_0 = 1 \text{ MeV}^4$ ; note that the plot barely changes for larger  $V_0$ .

55  $\mu\text{m}$ , as was also used in Ref. [64]. In addition, we follow Ref. [67] and assume the parallel plates to be surrounded by a residual hydrogen gas of temperature  $T = 300$  K and with a pressure of  $9.6 \times 10^{-10}$  mbar that is in thermal equilibrium with the plates and the light scalar fields. The resulting hydrogen mass density  $\rho_{\text{H}_2}$  determines the VEVs and masses of the considered screened scalar field models. Using these exemplary experimental conditions, the parts of the three models' parameter spaces that fulfill Eq. (41) are depicted in Fig. 2.

At first, we look at the  $n = 1$  chameleon. Taking into account  $\varphi_C \ll M_C$  and Eq. (41), we find that large parts of this model's parameter space allow for a thermal pressure at least as strong as the quantum pressure terms; see Fig. 2(a). Interestingly, the area depicted in Fig. 2(a) is entirely contained in the region that Ref. [64] constrains by solely using the chameleon quantum pressure. This means that the thermal pressure induced by chameleons is of experimental significance and must be taken into account.

Next, we look at the symmetron model. We only consider symmetrons in the symmetry-broken phase, in which the fifth force is not screened, and which is determined by the condition  $\mu^2 > \rho_{\text{H}_2}/M_S^2$ . Furthermore, we set  $\lambda_s = 0.1$  as Ref. [64] also did. In Fig. 2(b), we see

that also for large parts of the symmetron parameter space, the thermal pressure can be at least as strong as the quantum pressure.

Finally, we look at environment-dependent dilatons. Again, we find that large parts of the model parameter space allow for a thermal pressure that is significant in comparison to the quantum pressures. However, as of yet, nobody has computed quantum pressures for environment-dependent dilatons in specific experiments. Therefore, we cannot make a statement about the absolute magnitude of quantum and thermal pressures induced by this model. Such computations might be subject of a future work that takes into account a more realistic setup.

#### 4. Conclusions

Light scalar fields appear in many discussions throughout modern physics, and serve as candidates for dark energy or dark matter. While there are many experiments searching for evidence of such fields, there are physical aspects that are still not fully considered in experimental and theoretical analyses. A few years ago, Ref. [64] showed that the pressure induced by quantum fluctuations of screened scalar fields between two infinitely wide and infinitely thick plates can be of great

experimental importance. However, thermal pressures were not taken into account.

In the present article, we took first steps in the discussion of thermal pressures from light scalar fields. For this, we computed quantum and thermal potentials from one- and two-scalar exchanges between two nucleons. Next, we integrated these potentials over two thin but infinitely wide parallel plates, and subsequently derived expressions for quantum and thermal pressures from light scalar fields. Interestingly, we found that there is no thermal pressure from a single-particle exchange.

As explicit examples, we looked at three popular screened scalar field models: chameleons, symmetrons, and environment-dependent dilatons. Since we derived our general results for scalar fields with constant masses, we had to restrict our discussion to model parameters and experimental specifications for which the screened scalar fields cannot reach the minima of their potentials within each one of the two plates, such that we were allowed to set the scalar's VEVs and masses to the values corresponding to the density of the vacuum or gas the two plates are embedded in. Using an explicit experimental setup as an example, for all three considered screened scalar field models, we found large regions in their parameter spaces for which the thermal pressures are at least as significant as the quantum pressures. The region for the  $n = 1$  chameleon model is fully included in the area constrained in Ref. [64], which prompted us to conclude that chameleon thermal pressures are actually of experimental significance.

Our findings imply that re-evaluations of the chameleon and symmetron constraints presented in Ref. [64], that also take into account thermal pressures, might be necessary. However, this quite likely also applies to many other constraints on screened scalar fields, including environment-dependent dilatons, for which thermal effects were not taken into account. Therefore, we believe that finite-temperature effects must necessarily be discussed in future analyses of experiments that aim to constrain screened scalars or light scalar fields in general. For this, we must go beyond the initial steps taken here. This means that future analyses should make use of less assumptions than we did in ours. For example, if looking at screened scalar fields, the changes of VEVs and masses due to the presence of the two plates must be accurately described. In addition, the impact of the possible presence of a vacuum chamber or other experimental equipment should be taken into account and the assumption  $D \ll \ell$  might have to be dropped. However, in this case, analytical solutions can most likely not be obtained, which necessitates the use of sophisticated numerical methods.

### CRedit authorship contribution statement

**Hauke Fischer:** Writing – review & editing, Conceptualization. **Christian Käding:** Writing – review & editing, Writing – original draft, Visualization, Validation, Methodology, Investigation, Funding acquisition, Formal analysis, Data curation, Conceptualization. **Mario Pitschmann:** Writing – review & editing, Writing – original draft, Validation, Methodology, Investigation, Funding acquisition, Formal analysis, Conceptualization.

### Declaration of competing interest

The authors declare that they have no known competing financial interests or personal relationships that could have appeared to influence the work reported in this paper.

### Acknowledgments

This research was funded in whole or in part by the Austrian Science Fund (FWF) [10.55776/P34240], and [10.55776/PAT8564023], and is based upon work from COST Action COSMIC WISPerS CA21106, supported by COST (European Cooperation in Science and Technology). For open access purposes, the author has applied a CC BY public copyright license to any author accepted manuscript version arising from this submission. The authors acknowledge TU Wien Bibliothek, Austria for financial support through its Open Access Funding Programme.

### Data availability

Data will be made available on request.

### References

- [1] Y. Fujii, K.-i. Maeda, *The scalar-tensor theory of gravitation*, in: Cambridge Monographs on Mathematical Physics, Cambridge University Press, 2003.
- [2] T. Clifton, P.G. Ferreira, A. Padilla, C. Skordis, Modified gravity and cosmology, *Phys. Rep.* 513 (1) (2012) 1–189, [Modified Gravity and Cosmology](#).
- [3] A. Joyce, B. Jain, J. Khoury, M. Trodden, Beyond the cosmological standard model, *Phys. Rep.* 568 (2015) 1–98, [arXiv:1407.0059](#).
- [4] J.O. Dickey, P.L. Bender, J.E. Faller, X.X. Newhall, R.L. Ricklefs, J.G. Ries, P.J. Shelus, C. Veillet, A.L. Whipple, J.R. Wiant, J.G. Williams, C.F. Yoder, Lunar laser ranging: A continuing legacy of the apollo program, *Science* 265 (5171) (1994) 482–490.
- [5] E.G. Adelberger, B.R. Heckel, A.E. Nelson, Tests of the gravitational inverse-square law, *Annu. Rev. Nucl. Part. Sci.* 53 (1) (2003) 77–121.
- [6] D.J. Kapner, T.S. Cook, E.G. Adelberger, J.H. Gundlach, B.R. Heckel, C.D. Hoyle, H.E. Swanson, Tests of the gravitational inverse-square law below the dark-energy length scale, *Phys. Rev. Lett.* 98 (2007) 021101.
- [7] C. Burrage, E.J. Copeland, P. Millington, Radial acceleration relation from symmetron fifth forces, *Phys. Rev. D* 95 (6) (2017) 064050, [arXiv:1610.07529](#); *Phys. Rev. D* 95 (2017) 129902, Erratum.
- [8] C.A.J. O'Hare, C. Burrage, Stellar kinematics from the symmetron fifth force in the Milky Way disk, *Phys. Rev. D* 98 (6) (2018) 064019, [arXiv:1805.05226](#).
- [9] C. Burrage, E.J. Copeland, C. Käding, P. Millington, Symmetron scalar fields: Modified gravity, dark matter, or both? *Phys. Rev. D* 99 (4) (2019) 043539, [arXiv:1811.12301](#).
- [10] C. Käding, Lensing with generalized symmetrons, *Astronomy* 2 (2) (2023) 128–140, [arXiv:2304.05875](#).
- [11] J. Khoury, A. Weltman, Chameleon cosmology, *Phys. Rev. D* 69 (2004) 044026, [arXiv:astro-ph/0309411](#).
- [12] J. Khoury, A. Weltman, Chameleon fields: Awaiting surprises for tests of gravity in space, *Phys. Rev. Lett.* 93 (2004) 171104, [arXiv:astro-ph/0309300](#).
- [13] H. Dehnen, H. Frommert, F. Ghaboussi, Higgs field and a new scalar - tensor theory of gravity, *Internat. J. Theoret. Phys.* 31 (1992) 109–114.
- [14] E. Gessner, A new scalar tensor theory for gravity and the flat rotation curves of spiral galaxies, *Astrophys. Space Sci.* 196 (1) (1992) 29–43.
- [15] T. Damour, A.M. Polyakov, The String dilaton and a least coupling principle, *Nuclear Phys. B* 423 (1994) 532–558, [arXiv:hep-th/9401069](#).
- [16] M. Pietroni, Dark energy condensation, *Phys. Rev. D* 72 (2005) 043535.
- [17] K.A. Olive, M. Pospelov, Environmental dependence of masses and coupling constants, *Phys. Rev. D* 77 (2008) 043524.
- [18] P. Brax, C. van de Bruck, A.-C. Davis, D. Shaw, The dilaton and modified gravity, *Phys. Rev. D* 82 (2010) 063519, [arXiv:1005.3735](#).
- [19] K. Hinterbichler, J. Khoury, Symmetron fields: Screening long-range forces through local symmetry restoration, *Phys. Rev. Lett.* 104 (2010) 231301, [arXiv:1001.4525](#).
- [20] K. Hinterbichler, J. Khoury, A. Levy, A. Matas, Symmetron cosmology, *Phys. Rev. D* 84 (2011) 103521, [arXiv:1107.2112](#).
- [21] M. Gasperini, F. Piazza, G. Veneziano, Quintessence as a runaway dilaton, *Phys. Rev. D* 65 (2002) 023508, [arXiv:gr-qc/0108016](#).
- [22] T. Damour, F. Piazza, G. Veneziano, Violations of the equivalence principle in a dilaton runaway scenario, *Phys. Rev. D* 66 (2002) 046007, [arXiv:hep-th/0205111](#).
- [23] T. Damour, F. Piazza, G. Veneziano, Runaway dilaton and equivalence principle violations, *Phys. Rev. Lett.* 89 (2002) 081601, [arXiv:gr-qc/0204094](#).
- [24] P. Brax, C. van de Bruck, A.-C. Davis, B. Li, D.J. Shaw, Nonlinear structure formation with the environmentally dependent dilaton, *Phys. Rev. D* 83 (2011) 104026, [arXiv:1102.3692](#).
- [25] P. Brax, H. Fischer, C. Käding, M. Pitschmann, The environment dependent dilaton in the laboratory and the solar system, *Eur. Phys. J. C* 82 (10) (2022) 934, [arXiv:2203.12512](#).
- [26] C. Burrage, J. Sakstein, A compendium of chameleon constraints, *J. Cosmol. Astropart. Phys.* 11 (2016) 045, [arXiv:1609.01192](#).
- [27] Y.N. Kokotilovski, Strongly coupled chameleon fields: Possible test with a neutron Lloyd's mirror interferometer, *Phys. Lett. B* 719 (2013) 341–345, [arXiv:1203.5017](#).
- [28] Y.N. Kokotilovski, Potential of the neutron Lloyd's mirror interferometer for the search for new interactions, *J. Exp. Theor. Phys.* 116 (4) (2013) 609–619, [arXiv:1311.4679](#); *J. Exp. Theor. Phys.* 116 (2013) 886, Erratum.
- [29] T. Jenke, et al., Gravity resonance spectroscopy constrains dark energy and dark matter scenarios, *Phys. Rev. Lett.* 112 (2014) 151105, [arXiv:1404.4099](#).

- [30] S. Baum, G. Cantatore, D.H. Hoffmann, M. Karuza, Y.K. Semertzidis, A. Upadhye, K. Zioutas, Detecting solar chameleons through radiation pressure, *Phys. Lett. B* 739 (2014) 167–173, [arXiv:1409.3852](#).
- [31] C. Burrage, E.J. Copeland, E.A. Hinds, Probing dark energy with atom interferometry, *J. Cosmol. Astropart. Phys.* 03 (2015) 042, [arXiv:1408.1409](#).
- [32] P. Hamilton, M. Jaffe, P. Haslinger, Q. Simmons, H. Müller, J. Khoury, Atom-interferometry constraints on dark energy, *Science* 349 (2015) 849–851, [arXiv:1502.03888](#).
- [33] H. Lemmel, P. Brax, A.N. Ivanov, T. Jenke, G. Pignol, M. Pitschmann, T. Potocar, M. Wellenzohn, H. Abele, Neutron Interferometry constrains dark energy chameleon fields, *Phys. Lett. B* 743 (2015) 310–314, [arXiv:1502.06023](#).
- [34] C. Burrage, E.J. Copeland, Using atom interferometry to detect dark energy, *Contemp. Phys.* 57 (2) (2016) 164–176, [arXiv:1507.07493](#).
- [35] B. Elder, J. Khoury, P. Haslinger, M. Jaffe, H. Müller, P. Hamilton, Chameleon dark energy and atom interferometry, *Phys. Rev. D* 94 (4) (2016) 044051, [arXiv:1603.06587](#).
- [36] A.N. Ivanov, G. Cronenberg, R. Höllwieser, M. Pitschmann, T. Jenke, M. Wellenzohn, H. Abele, Exact solution for chameleon field, self-coupled through the Ratra-Peebles potential with  $n = 1$  and confined between two parallel plates, *Phys. Rev. D* 94 (8) (2016) 085005, [arXiv:1606.06867](#).
- [37] C. Burrage, A. Kuribayashi-Coleman, J. Stevenson, B. Thrussell, Constraining symmetron fields with atom interferometry, *J. Cosmol. Astropart. Phys.* 12 (2016) 041, [arXiv:1609.09275](#).
- [38] M. Jaffe, P. Haslinger, V. Xu, P. Hamilton, A. Upadhye, B. Elder, J. Khoury, H. Müller, Author Correction: Testing sub-gravitational forces on atoms from a miniature in-vacuum source mass [doi: 10.1038/nphys4189], *Nat. Phys.* 13 (2017) 938, [arXiv:1612.05171](#).
- [39] P. Brax, M. Pitschmann, Exact solutions to nonlinear symmetron theory: One- and two-mirror systems, *Phys. Rev. D* 97 (6) (2018) 064015, [arXiv:1712.09852](#).
- [40] D.O. Sabulsky, I. Dutta, E.A. Hinds, B. Elder, C. Burrage, E.J. Copeland, Experiment to detect dark energy forces using atom interferometry, *Phys. Rev. Lett.* 123 (6) (2019) 061102, [arXiv:1812.08244](#).
- [41] P. Brax, C. Burrage, A.-C. Davis, Laboratory constraints, *Internat. J. Modern Phys. D* 27 (15) (2018) 1848009.
- [42] G. Cronenberg, P. Brax, H. Filter, P. Geltenbort, T. Jenke, G. Pignol, M. Pitschmann, M. Thalhammer, H. Abele, Acoustic Rabi oscillations between gravitational quantum states and impact on symmetron dark energy, *Nat. Phys.* 14 (10) (2018) 1022–1026, [arXiv:1902.08775](#).
- [43] D. Hartley, C. Käding, R. Howl, I. Fuentes, Quantum simulation of dark energy candidates, *Phys. Rev. D* 99 (10) (2019) 105002, [arXiv:1811.06927](#).
- [44] X. Zhang, R. Niu, W. Zhao, Constraining the scalar-tensor gravity theories with and without screening mechanisms by combined observations, *Phys. Rev. D* 100 (2) (2019) 024038, [arXiv:1906.10791](#).
- [45] S. Arguedas Cuendis, et al., First results on the search for chameleons with the KWISP detector at CAST, *Phys. Dark Univ.* 26 (2019) 100367, [arXiv:1906.01084](#).
- [46] T. Jenke, J. Bosina, J. Micko, M. Pitschmann, R. Sedmik, H. Abele, Gravity resonance spectroscopy and dark energy symmetron fields: qBOUNCE experiments performed with Rabi and Ramsey spectroscopy, *Eur. Phys. J. ST* 230 (4) (2021) 1131–1136, [arXiv:2012.07472](#).
- [47] M. Pitschmann, Exact solutions to nonlinear symmetron theory: One- and two-mirror systems. II, *Phys. Rev. D* 103 (8) (2021) 084013, [arXiv:2012.12752](#); *Phys. Rev. D* 106 (2022) 109902, Erratum.
- [48] P. Brax, S. Casas, H. Desmond, B. Elder, Testing screened modified gravity, *Universe* 8 (1) (2021) 11, [arXiv:2201.10817](#).
- [49] S. Qvarfort, D. Rätzl, S. Stopyra, Constraining modified gravity with quantum optomechanics, *New J. Phys.* 24 (3) (2022) 033009, [arXiv:2108.00742](#).
- [50] P. Yin, R. Li, C. Yin, X. Xu, X. Bian, H. Xie, C.-K. Duan, P. Huang, J.-h. He, J. Du, Experiments with levitated force sensor challenge theories of dark energy, *Nat. Phys.* 18 (10) (2022) 1181–1185.
- [51] J. Betz, J. Manley, E.M. Wright, D. Grin, S. Singh, Searching for chameleon dark energy with mechanical systems, *Phys. Rev. Lett.* 129 (13) (2022) 131302, [arXiv:2201.12372](#).
- [52] P. Brax, A.-C. Davis, B. Elder, Screened scalar fields in hydrogen and muonium, *Phys. Rev. D* 107 (4) (2023) 044008, [arXiv:2207.11633](#).
- [53] D. Hartley, C. Käding, R. Howl, I. Fuentes, Quantum-enhanced screened dark energy detection, *Eur. Phys. J. C* 84 (1) (2024) 49, [arXiv:1909.02272](#).
- [54] H. Fischer, C. Käding, R.I.P. Sedmik, H. Abele, P. Brax, M. Pitschmann, Search for environment-dependent dilatons, *Phys. Dark Univ.* 43 (2024) 101419, [arXiv:2307.00243](#).
- [55] H. Fischer, C. Käding, H. Lemmel, S. Sponar, M. Pitschmann, Search for dark energy with neutron interferometry, *PTEP* 2024 (2) (2024) 023E02, [arXiv:2310.18109](#).
- [56] H. Fischer, R.I.P. Sedmik, Numerical Methods for Scalar Field Dark Energy in Table-top Experiments and Lunar Laser Ranging, *JCAP* 10 (2024) 026.
- [57] G.L. Klimchitskaya, V.M. Mostepanenko, The nature of dark energy and constraints on its hypothetical constituents from force measurements, *Universe* 10 (3) (2024) 119, [arXiv:2403.05988](#).
- [58] H. Haghmoradi, H. Fischer, A. Bertolini, I. Galí, F. Intraiva, M. Pitschmann, R. Schimpl, R.I.P. Sedmik, Force metrology with plane parallel plates: Final design review and outlook, *MDPI Phys.* 6 (2) (2024) [arXiv:2403.10998](#).
- [59] A.L. Báez-Camargo, D. Hartley, C. Käding, I. Fuentes-Guridi, Dynamical Casimir effect with screened scalar fields, *AVS Quantum Sci.* 6 (2024) 045001.
- [60] T. O’Shea, A.-C. Davis, M. Giannotti, S. Vagnozzi, L. Visinelli, J.K. Vogel, Solar chameleons: novel channels (I), *Phys. Rev. D* 110 (2024) 063027.
- [61] C.D. Panda, M.J. Trao, M. Ceja, J. Khoury, G.M. Tino, H. Müller, Measuring gravitational attraction with a lattice atom interferometer, *Nature* (2024) [arXiv:2310.01344](#).
- [62] H. Fischer, C. Käding, M. Pitschmann, Screened scalar fields in the laboratory and the solar system, *Universe* 10 (7) (2024) 297, [arXiv:2405.14638](#).
- [63] C. Burrage, J. Sakstein, Tests of chameleon gravity, *Living Rev. Rel.* 21 (1) (2018) 1, [arXiv:1709.09071](#).
- [64] P. Brax, S. Ficht, Quantum chameleons, *Phys. Rev. D* 99 (10) (2019) 104049, [arXiv:1809.10166](#).
- [65] C. Burrage, C. Käding, P. Millington, J. Minář, Open quantum dynamics induced by light scalar fields, *Phys. Rev. D* 100 (7) (2019) 076003, [arXiv:1812.08760](#).
- [66] C. Burrage, C. Käding, P. Millington, J. Minář, Influence functionals, decoherence and conformally coupled scalars, *J. Phys. Conf. Ser.* 1275 (1) (2019) 012041, [arXiv:1902.09607](#).
- [67] C. Käding, M. Pitschmann, C. Voith, Dilaton-induced open quantum dynamics, *Eur. Phys. J. C* 83 (8) (2023) 767, [arXiv:2306.10896](#).
- [68] S. Sevillano Muñoz, A particle’s perspective on screening mechanisms, 2024, [arXiv:2407.08779](#).
- [69] R.I.P. Sedmik, M. Pitschmann, Next generation design and prospects for cannex, *Universe* 7 (7) (2021) 234, [arXiv:2107.07645](#).
- [70] P. Brax, A.-C. Davis, Casimir, gravitational and neutron tests of dark energy, *Phys. Rev. D* 91 (6) (2015) 063503, [arXiv:1412.2080](#).
- [71] A. Almasi, P. Brax, D. Iannuzzi, R.I.P. Sedmik, Force sensor for chameleon and Casimir force experiments with parallel-plate configuration, *Phys. Rev. D* 91 (10) (2015) 102002, [arXiv:1505.01763](#).
- [72] B. Elder, V. Vardanyan, Y. Akrami, P. Brax, A.-C. Davis, R.S. Decca, Classical symmetron force in Casimir experiments, *Phys. Rev. D* 101 (6) (2020) 064065, [arXiv:1912.10015](#).
- [73] P. Brax, A.-C. Davis, B. Elder, Casimir tests of scalar-tensor theories, *Phys. Rev. D* 107 (8) (2023) 084025, [arXiv:2211.07840](#).
- [74] M. Pitschmann, The High Precision Frontier: Search for New Physics with “Tabletop Experiments” & Beyond (Ph.D. thesis), TU Wien, 2023.
- [75] F. Ferrer, M. Nowakowski, Higgs and Goldstone bosons mediated long range forces, *Phys. Rev. D* 59 (1999) 075009, [arXiv:hep-ph/9810550](#).
- [76] G. Feinberg, J. Sucher, C.K. Au, The dispersion theory of dispersion forces, *Phys. Rep.* 180 (1989) 83.
- [77] F. Ferrer, J.A. Grifols, M. Nowakowski, Long range forces induced by neutrinos at finite temperature, *Phys. Lett. B* 446 (1999) 111–116, [arXiv:hep-ph/9806438](#).
- [78] C.J. Horowitz, J.T. Pantaleone, Long range forces from the cosmological neutrinos background, *Phys. Lett. B* 319 (1993) 186–190, [arXiv:hep-ph/9306222](#).